Electronic structure of M_3^{I}Sb-type filled tetrahedral semiconductors

Su-Huai Wei and Alex Zunger
Solar Energy Research Institute, Golden, Colorado 80401
(Received 22 October 1986)

First-principles band-structure and total-energy calculations have been performed for Li_3Sb, K_3Sb, and Cs_3Sb in the cubic $D0_3$ structure. The structure of these $M_3^{\mathrm{I}}A^{\mathrm{V}}$ octet semiconductors consists of a face-centered-cubic lattice A^{V} in which three metal M^{I} atoms occupy the interstitial sites, thereby completing the octet shell. The equilibrium lattice parameters and bulk moduli calculated from the total energy agree well with available experimental data. The semiconducting character of K_3Sb and Cs_3Sb is attributed to p-d repulsion between the anion p states and the unoccupied metal d states. The calculated charge density shows weak covalent bonding between like atoms and ionic bonding between unlike atoms. The covalency decreases and the ionicity increases with increasing metal atomic number, as the M^+ cores dilate the lattice. We find that the electronic structure of these compounds can be understood qualitatively by considering a skeleton of Sb^{3-} anions whose separation is determined by the otherwise nearly inert alkali ions M^+. The trends in the electronic properties in the series M=Li, K, and Cs then reflect the perturbations exerted by different M^+ ions through (i) charge transfer, (ii) p-d hybridization, and (iii) relativistic effects.

I. INTRODUCTION

Combination of the alkali metals (M) with antimony yields a group of interesting semiconductors which attracted considerable attention in past years.[1] These materials possess relatively small electron affinities and high photoelectric quantum efficiencies in the visible region.[1,2] As high-sensitivity photocathod materials, these compounds have been widely utilized in photometry, optical image, and other device applications.[1]

Studies[1] of the chemical composition, and x-ray and electron diffraction reveal that alkali-antimony compounds have the stoichiometric composition M_3Sb (where M can be one or more types of alkali-metal elements), crystallize either in (i) the hexagonal Na_3As structure (space group D_{6h}^4), (ii) the cubic (or, β) modification of the BiF_3 structure (space group O_h^5, or the $D0_3$ structure, see inset to Fig. 1), or (iii) the partially disordered NaTl structure (space group O_h^7). The high photosensitivity[3] of these systems is found in the cubic structure and has been attributed to band bending caused by a dipole layer at the surface of these highly electropositive systems.

Despite the large variations in atom size and properties of the different alkali elements in M_3Sb and the resulting dramatic changes in lattice constants of the compounds[4-6] (a=6.572 Å for β-Li_3Sb, a=8.493 Å for K_3Sb, and a=9.128 Å for Cs_3Sb), all the alkali-antimony compounds are semiconductors[1] with surprisingly small variations of the band gap (all within 1.0–1.6 eV).[1,3] This is rather unexpected since conventional volume (V) deformation potentials of band gaps $-dE_g/d\ln V$ (ranging[7] between 7 and 30 eV) would suggest that the larger-volume M_3Sb compounds (e.g., K_3Sb, Cs_3Sb) might be metallic. Theoretical[8] and experimental[9] studies also indicate that the top of the valence bands for M_3Sb (except for Li_3Sb) is nearly dispersionless, a characteristic of ionic insulators, not semiconductors. The nature of the chemical bonding in M_3Sb, i.e., whether they are ionic, covalent, or "charge-transfer semiconductors,"[10] has similarly been a subject of ongoing theoretical[10,11] and experimental investigation.[12,13] (This subject is also of current interest because of its relation to the metal-nonmetal transition observed in several liquid alkali-pnictogen alloys.[14]) A few propositions have been advanced: the cubic crystal structure of β-M_3Sb and the valences of M and Sb (one and five, respectively) have suggested to Suchet[15] an "interstitial compensatory lattice model" in which the antimony atom and its nearest-neighbor alkali atoms (denoted M_{II}) form a covalently bonded lattice through s-p hybridization; the role of the other alkali atom (denoted M_{I}) is then to provide one extra electron to compensate the covalent bond. This suggests that these compounds have the pseudo-face-centered ionic form $[M_{\mathrm{II}}\mathrm{Sb}M_{\mathrm{II}}]^{-1}M_{\mathrm{I}}{}^{+1}$. However, x-ray photoemission studies[13] indicated for Cs_3Sb only a single type of Cs atom (predominantly in the Cs^+ form), in conflict with this model. Recently, Robertson,[10] using the tight-binding method, has performed calculations for Li_3Sb and Cs_3Sb in an attempt to determine whether the chemical bonding is predominantly covalent or ionic. Based on his calculation of the ionicities (defined loosely as the atomic charge on the cation) he found that M_3Sb could be viewed as a "charge-transfer semiconductor" whose ionicity could be quite small due to the delocalization of the Sb orbitals. A study by Christensen[11] indicates that, because of the large differences in size of the alkali atoms, remarkable differences in bonding exist between Li_3Sb and Cs_3Sb. He suggests that Li_3Sb resembles a molecular crystal but that Cs_3Sb appears to be dominated by ionic bonding, similar to that in CsI. The band structure for Cs_3Sb has also been calculated by Nishikawa *et al.*[16] using the augmented-plane-wave method.

In this paper we have performed systematic first-principles total-energy and band-structure calculations for

β-M_3Sb (M=Li,K,Cs) in the ordered cubic $D0_3$ structure. In this crystal structure (inset to Fig. 1), four simple face-centered sublattices are mutually displaced along the body diagonal such that all nearest-neighbor distances equal $\frac{1}{4}$ of this diagonal. There are two different types of crystallographically inequivalent cations in this structure: $M_{\rm I}$ with eight $M_{\rm II}$ cation as nearest neighbors, and $M_{\rm II}$ with four cations and four anions as nearest neighbors. The primitive lattice vectors are

$$\mathbf{a}_1=(0,\tfrac{1}{2},\tfrac{1}{2})a\ ,\quad \mathbf{a}_2=(\tfrac{1}{2},0,\tfrac{1}{2})a\ ,\quad \mathbf{a}_3=(\tfrac{1}{2},\tfrac{1}{2},0)a\ , \tag{1}$$

and the atomic site coordinates are as follows: Sb at

$$\tau_1=(0,0,0)a\ ,$$

$M_{\rm II}$ at

$$\tau_2=(\tfrac{1}{4},\tfrac{1}{4},\tfrac{1}{4})a\ ,$$

$M_{\rm I}$ at

$$\tau_3=(\tfrac{1}{2},\tfrac{1}{2},\tfrac{1}{2})a\ , \tag{2}$$

and $M_{\rm II}$ at

$$\tau_4=(\tfrac{3}{4},\tfrac{3}{4},\tfrac{3}{4})a\ ,$$

where a is the cubic lattice constant.

From total-energy calculations we have obtained the ground-state properties of these systems. The band structures of Li_3Sb, K_3Sb, Cs_3Sb, and that for a hypothetical crystal $(Sb^{3-})^{3+}$ (with three additional positive charges uniformly distributed in the unit cell for charge neutrality) have isolated three physical contributions to the electronic structure: (i) lattice relaxation, (ii) p-d repulsion, and (iii) the relativistic effects. The chemical bonding in these compounds has been studied through charge-density plots.

II. METHOD OF CALCULATION

The total-energy and electronic band structures are calculated with use of the first-principles self-consistent general-potential linearized augmented-plane-wave (LAPW) method[17] within the local-density-functional formalism.[18] Several exchange-correlation functional forms[19–21] have been used to test the dependence of ground-state properties (lattice constant, bulk modulus) on these potentials. Scalar relativistic effects (i.e., including directly all relativistic effects but the spin-orbit coupling) are incorporated for all valence states; spin-orbit coupling is included only in the calculation of the splitting Δ_0 of the Γ_{15v} states at the valence-band maximum. Core states have been calculated fully relativistically in a spherical approximation. All core and valence states are calculated self-consistently without invoking the frozen-core approximation. Shape unrestricted potentials and charge densities are used throughout. The two special **k** points of Chadi and Cohen[22] are used for the Brillouin-zone integration. The basis set consists of about 200 functions (a basis set of about 300 functions was, however, needed for the calculations which treat Cs $5p$ states as valence states, see below). Eigenvalues of the valence states are converged to better than 0.03 eV (0.2 mRy). Finally, the density of states (DOS) is calculated using the tetrahedral integration method[23] with a square broadening scheme (with a width of 0.16 eV, or 12 mRy) and eight primary **k** points.

III. RESULTS AND DISCUSSION

A. Total-energy and ground-state properties

The total and cohesive energies as a function of lattice parameter were calculated for Li_3Sb, K_3Sb, and Cs_3Sb in the cubic (β) $D0_3$ structure and are depicted in Fig. 1. The calculated total energies using the Wigner[19] interpolation formula at three values of the lattice parameter were fitted to a quadratic form and interpolated to obtain the zero-temperature equilibrium lattice constant $a_{\rm eq}$ and bulk modulus B. The cohesive energies, using the Von Barth—Heding spin-polarized exchange correlation potential (in the Hedin-Lundquist paramagnetic limit), are obtained by subtracting the spin-unrestricted atomic total

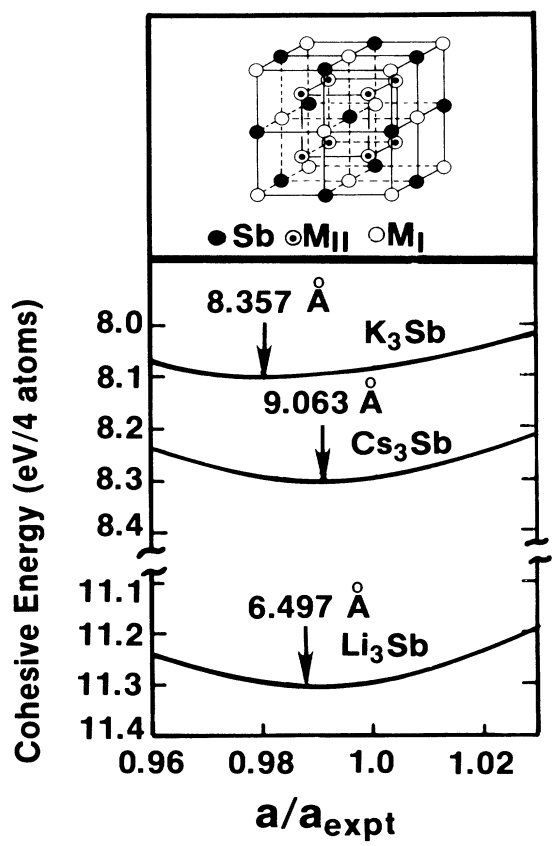

FIG. 1. Cohesive energy per unit cell as a function of relative lattice constant ($a/a_{\rm expt}$) for Li_3Sb, K_3Sb, and Cs_3Sb. $a_{\rm expt}$ is the experimental lattice constant (see Table I). Arrow indicates the calculated equilibrium. The Wigner (Ref. 19) interpolation formula is used. The inset depicts the $D0_3$ crystal structure.

TABLE I. Calculated [using the Wigner (Ref. 19) exchange-correlation functional] equilibrium lattice constants (a_{eq}), bulk moduli (B), cohesive energy per four atoms (E_c) and spin-orbit splitting of the valence-band maximum (Δ_0) of Li_3Sb, K_3Sb, and Cs_3Sb in the $D0_3$ structure, compared with experimental data and the LMTO results of Christensen (Ref. 11) [using the Ceperley-Alder (Ref. 21) exchange correlation].

	Li_3Sb			K_3Sb		Cs_3Sb		
Properties	Present calc.	LMTO[a]	Exptl.	Present calc.	Exptl.	Present calc.	LMTO[a]	Exptl.
a_{eq} (Å)	6.497	6.631[b]	6.572[c]	8.357	8.493[e]	9.063	9.415[b]	9.128[f]
B (kbar)	344	343		148		140	151	
E_c (eV)	11.3		9.32[d]	8.1	7.50[d]	8.3		
Δ_0 (eV)	0.62			0.43		0.42		

[a]Reference 11.
[b]These rather large lattice parameters are the results published in Ref. 11, where the calculations were performed in the atomic-sphere approximation (ASA). Christensen believes (Ref. 29) that upon improving this approximation, the lattice parameters of Li_3Sb and Cs_3Sb would be reduced to 6.52 and 9.24 Å, respectively.
[c]Reference 4.
[d]Reference 25.
[e]Reference 5.
[f]Reference 6.

energies (including spin-polarization corrections which are 0.37, 0.25, 0.21, and 1.35 eV for Li, K, Cs, and Sb, respectively) from the crystal total energies. The calculated cohesive energies are assumed to be independent of specific correlation form. These results are summarized in Table I where they are compared with the experimental data[24,25] and with the linear—muffin-tin-orbital (LMTO) results of Christensen[11,26] for Li_3Sb and Cs_3Sb. In our calculation for Cs_3Sb we treat the partially delocalized Cs $5p$ states as variational valence-band states, i.e., on the same footing as all the other valence electrons. We find that treating the $5p$ states as dispersionless core states (but self-consistently) gives a lattice constant which is about 3.5% too small.[26] We find that our calculated lattice constants are systematically smaller than the observed ones. (This can partially be attributed to thermal expansion; our results correspond to 0 K.) Our results indicate that bulk K_3Sb and Cs_3Sb are very soft compared to conventional semiconductors ($B \approx 400-1000$ kbar),[24] whereas Li_3Sb is more than twice as hard. The calculated cohesive energies E_c are about 1—2 eV larger than the experimental values,[25] a common situation for local-density calculations which neglect dynamical correlation (e.g., multiplet effects[21]). The larger cohesive energy of Cs_3Sb relative to K_3Sb is probably due to the additional bonding through the low-lying delocalized Cs $5p$ orbitals, which could increase the binding energy of Cs_3Sb by about 0.9 eV.[11] The larger p-d repulsion in Cs_3Sb (see below) also contributes to the increased cohesion of Cs_3Sb.

The dependence of the calculated ground-state properties on the exchange-correlation energy has been examined. Wigner's[19] interpolation formula (W), the Hedin-Lundqvist[20] correlation (HL) and the Ceperley-Alder correlation (CA) formula as parametrized by Perdew and Zunger[21] have been used to calculate ground-state properties for Li_3Sb. We find $a_{eq}=6.497$, 6.403, and 6.407 Å using the W, HL, and CA correlation energies, respectively. The changes in the bulk moduli are within 6% for all types of correlation energies. This general trend (i.e., a 1% larger lattice constant with the Wigner correlation relative to HL and CA) has been found previously for III-V compound semiconductors and other materials.[27]

B. Band structure and density of states

Calculated band structures of Li_3Sb, K_3Sb, and Cs_3Sb (using the Wigner exchange correlation) at their observed lattice parameters are depicted in Figs. 2(a)—2(c) along some high-symmetry lines. The total density of states and angular momentum and site projected local density of states are given in Figs. 3(a)—3(c). Eigenvalues and l-decomposed local charge characters at high symmetry points are listed in Table II.

All three compounds are semiconductors with band structures that show an overall similarity to those of III-V or II-VI systems. The lowest (L_{1v}-Γ_{1v}-X_{1v}) valence band, in all cases, is an Sb $5s$ band, separated by a heteropolar gap from the upper valence band (an Sb $5p$ band for Li_3Sb; an Sb $5p$—metal d band for K_3Sb and Cs_3Sb). The conduction bands are a mixture of Sb $4d$ and metal s,p orbitals (see Table II).

For Li_3Sb we find the lower valence band (VB) to be located at $E_v-9.3$ eV (where E_v is the Γ_{15v} valence-band maximum) with a bandwidth of 0.9 eV. The upper valence bands have a width of 3.7 eV. The spin-orbit splitting at the valence-band maximum (VBM) is 0.62 eV. The conduction bands (CB) are a mixture of the Li $2s$, $2p$ and the Sb $4d$ states. The indirect (I) band gap is $E_g^I=0.74$ eV, whereas the direct (D) band gap (at Γ) is $E_g^D=2.20$ eV. The experimental situation concerning the band gap of Li_3Sb is not clear. The estimated band gap is about[28] 2.9 eV, which we think might be the direct transition. (The small calculated band gap is a general feature of the local density formalism.[21]) The calculated LMTO gap E_g^I of Ref. 11 is 0.74 eV (0.14 eV was cited erroneously).[29] There is an overall topological resemblance of the band structure calculated by Christensen[11] and the present results.

For K_3Sb, the width of the valence states is consider-

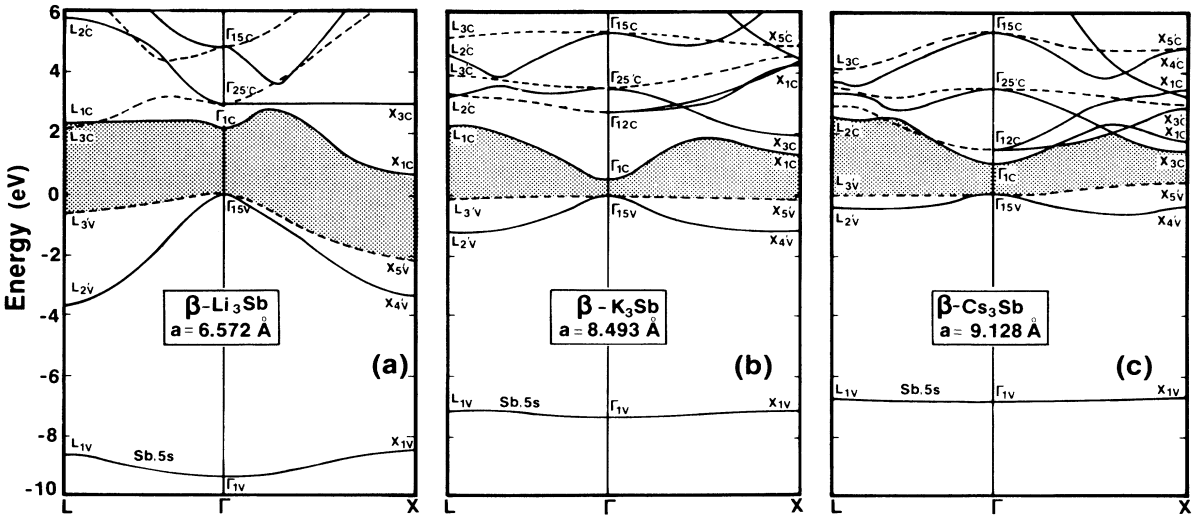

FIG. 2. Band structures of cubic (a) Li_3Sb, (b) K_3Sb, and (c) Cs_3Sb calculated with the Wigner (Ref. 19) exchange-correlation at the experimental lattice constants. The origin of the coordinate system is at the Sb site. The band-gap regions are shaded. Dashed lines indicate doubly degenerate states. The Cs $5p$ (semicore) bands are not shown in this plot.

ably smaller. The lower valence band is located at $E_v - 7.31$ eV, with a band width of only 0.2 eV. The upper valence band is similarly narrow (1.26 eV wide). The highest valence band ($L_{3'v}$-Γ_{15v}-$X_{5'v}$) is almost dispersionless. The calculated spin-orbit splitting Δ_0 is 0.43 eV at the valence-band maximum (VBM). Our results, therefore, do not agree with an estimation of Δ_0 as about 0.7 eV of Ref. 30. We find this material to be a direct- (Γ_{1c}-Γ_{15v}) band-gap semiconductor. The calculated direct band gap $E_g^D = 0.56$ eV is smaller than the experimental value of[5] 1.4 eV. Compared with the conduction bands of Li_3Sb, those of K_3Sb are more complicated due

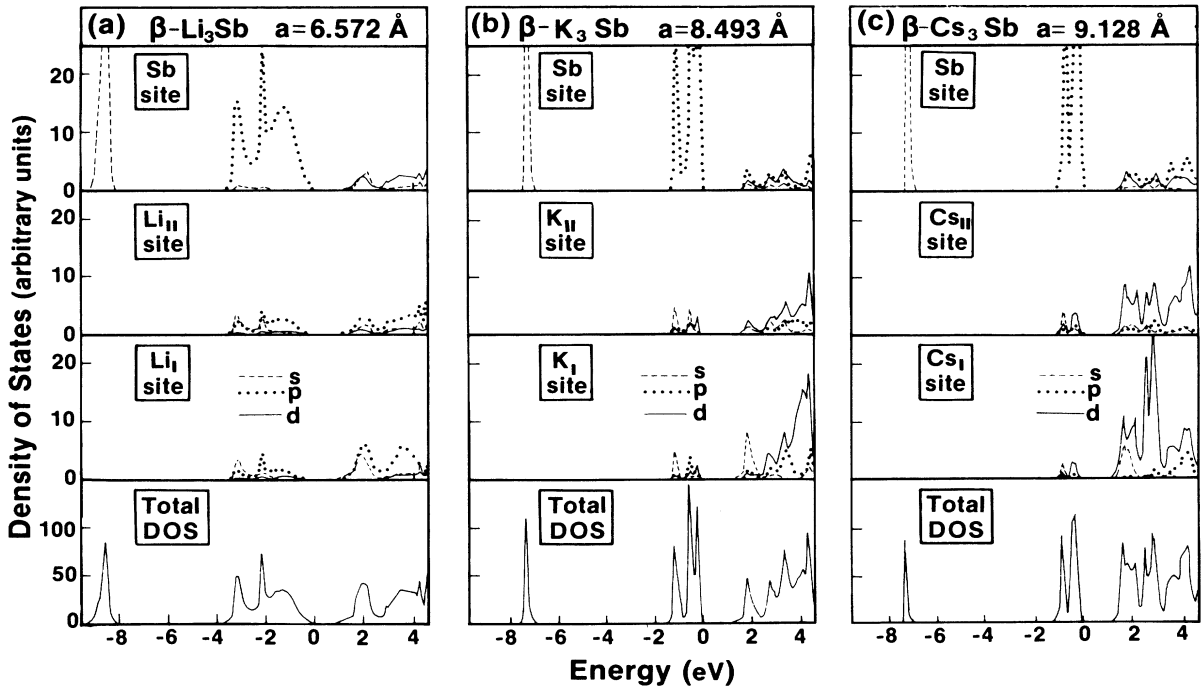

FIG. 3. Total density of states (DOS), and angular-momentum and site projected local DOS of (a) Li_3Sb, (b) K_3Sb, and (c) Cs_3Sb. For the local DOS, the dashed lines are the s component, the dotted lines are the p component, and the solid lines are the d component. The zero of energy is at the VBM.

TABLE II. Calculated [using Wigner's exchange correlation (Ref. 19)] one-electron eigenvalues (in eV) and l-decomposed local charge character (in percentages) inside atomic muffin-tin (MT) spheres of cubic Li_3Sb ($a=6.572$ Å, $R_{MT}=1.370$ Å), K_3Sb ($a=8.493$ Å, $R_{MT}=1.767$ Å, and Cs_3Sb ($a=9.128$ Å, $R_{MT}=1.900$ Å) at high-symmetry points. For each state the l characters are given for Sb (first row), M_I (second row), and M_{II} (third row). The energy zero is at the Γ_{15v} valence-band maximum.

	Li_3Sb				K_3Sb				Cs_3Sb			
State	ε	s	p	d	ε	s	p	d	ε	s	p	d
Γ_{1v}	−9.31	63	0	0	−7.31	85	0	0	−6.94	90	0	0
		3	0	0		1	0	0		0	0	0
		5	0	0		2	0	0		1	0	0
Γ_{15v}	0	0	57	0	0	0	62	0	0	0	62	0
		0	5	0		0	2	0		0	3	0
		0	1	3		0	1	6		0	0	7
Γ_{1c}	2.20	28	0	0	0.56	13	0	0	1.02	9	0	0
		25	0	0		25	0	0		22	0	0
		10	0	0		14	0	0		14	0	0
Γ_{12c}	7.28	0	0	19	2.81	0	0	8	1.47	0	0	6
		0	0	9		0	0	22		0	0	21
		0	0	9		0	0	17		0	0	17
$\Gamma_{25'c}$	2.98	0	0	11	3.60	0	0	6	3.53	0	0	2
		0	0	5		0	0	32		0	0	49
		0	23	0		0	13	0		0	7	4
Γ_{15c}	4.92	0	4	0	5.41	0	13	0	5.37	0	19	0
		0	35	0		0	23	0		0	14	0
		0	13	1		0	5	12		0	2	18
X_{1v}	−8.42	74	0	0	−7.11	89	0	0	−6.81	92	0	0
		1	0	1		0	0	0		0	0	0
		0	3	1		0	1	1		0	0	1
$X_{4'v}$	−3.27	0	32	0	−1.09	0	43	0	−0.46	0	52	0
		0	8	0		0	5	0		0	3	0
		11	0	1		9	0	2		6	0	2
$X_{5'v}$	−2.12	0	37	0	−0.06	0	60	0	0.40	0	69	0
		0	8	0		0	3	0		0	3	0
		0	10	0		0	5	1		0	2	2
X_{1c}	0.74	6	0	5	1.39	0	0	5	1.75	1	0	5
		30	0	0		34	0	0		23	0	5
		0	8	2		0	6	6		0	2	13
X_{3c}	3.07	0	0	11	2.01	0	0	7	1.43	0	0	5
		0	0	5		0	0	19		0	0	23
		21	0	2		14	0	7		9	0	10
L_{1v}	−8.67	70	0	0	−7.14	88	0	0	−6.82	92	0	0
		0	2	0		0	0	0		0	0	0
		2	2	0		0	1	0		0	0	0
$L_{2'v}$	−3.74	0	29	0	−1.26	0	38	0	−0.45	0	48	0
		11	0	0		10	0	1		6	0	2
		7	4	0		7	3	0		6	2	0
$L_{3'v}$	−0.63	0	51	0	−0.10	0	60	0	−0.07	0	56	0
		0	0	2		0	0	4		0	0	6
		0	7	2		0	2	3		0	1	5
L_{1c}	2.29	15	0	5	2.33	6	0	4	3.27	3	0	7
		0	17	0		0	13	0		0	10	0
		13	2	1		17	3	0		15	2	1
L_{3c}	2.22	0	0	8	3.39	0	0	8	3.47	0	0	7
		0	24	0		0	16	0		0	6	0
		0	13	2		0	6	11		0	3	18

to the presence of the unoccupied K $3d$ orbitals. These d orbitals have an important role in determining the structure of the upper valence band, the band gap, and the spin-orbit splitting at the VBM. This will be discussed in more detail in the following section. We also find a noticeable separation between the lowest CB (L_{1c}-Γ_{1c}-X_{1c}) and the upper CB at about 1.5 eV above the conduction-band minimum.

For Cs_3Sb, the band structure is very similar to that of K_3Sb, except that the valence band is even narrower. The Cs $5p$ core states are found at 3.1 and 2.0 eV below the bottom (Γ_{1v}) of the valence band for $Cs_{\rm I}$ and $Cs_{\rm II}$ ions, respectively (i.e., at $\varepsilon_v-10.0$ eV and $\varepsilon_v-8.9$ eV, respectively). The different $5p$ levels are due to the different local environments of the two types of Cs ions in the crystal. The lowest valence band is located at $E_v-6.94$ eV and its bandwidth is only 0.13 eV. The upper valence bands have a width of 0.86 eV. Our calculated Δ_0 for Cs_3Sb is 0.42 eV. This material has a calculated indirect band gap of $E_g^I=0.62$ eV. The VBM is located at $X_{5'v}$ and the CBM is at Γ_{1c}. The direct band gaps at Γ and X are 1.02 and 1.03 eV, respectively. Experimentally,[3,31] a band gap of 1.6 eV was measured for a partially disordered phase of Cs_3Sb (with O_h^7 symmetry) at 300 K. The LMTO results[11,29] for the indirect band gap is 0.52 eV (1.04 eV was reported erroneously[29] in Ref. 11).

C. The physics of chemical trends in M_3Sb band structures

1. Volume dilation effects

To understand the physical factors deciding the chemical trends in the band structures of M_3Sb (Fig. 2) we have calculated the band structure of a hypothetical $(Sb^{3-})^{3+}$ crystal in the face-centered-cubic structure, at the observed lattice parameters of the actual M_3Sb compounds (Fig. 4). To preserve electrical neutrality, we have added a uniform background of three positive charges. Table III compares the results to those obtained for actual M_3Sb compounds. As the lattice parameter increases in the M=Li→M=K→M=Cs sequence, the band structure of $(Sb^{3-})^{3+}$ shows the following. (i) A reduced width of the lower, (L_{1v}-Γ_{1v}-X_{1v}) Sb $4s$ band as well as of the upper valence band. This effect is simply due to a reduced Sb-Sb overlap with increasing lattice constant. (ii) Since the volume deformation potentials $-dE_g(\Gamma_{15v}\rightarrow\Gamma_{1c})/d\ln V$ and $-dE_g(\Gamma_{15v}\rightarrow L_{1c})/d\ln V$ of tetrahedral semiconductors are *positive*,[32] but that of $-dE_g(\Gamma_{15v}\rightarrow X_{1c})/d\ln V$ is *negative*,[32] a volume increase along the Li_3Sb →K_3Sb→Cs_3Sb sequence *reduces* the $\Gamma_{15v}\rightarrow\Gamma_{1c}$, and $\Gamma_{15v}\rightarrow L_{1c}$ band gaps, but *raises* the $\Gamma_{15v}\rightarrow X_{1c}$ band gap. Hence, the "directness" of the band gap increases in the Li→K→Cs sequence simply due to volume dilation effects. Table III and the comparison of Fig. 4 to Fig. 2 indicate that the electronic structure of M_3Sb compounds, to zero order, is that of an $(Sb^{3-})^{3+}$ structure with Sb-Sb separations determined by the type of cation.

2. p-d repulsion effects

We next consider effects omitted by the $(Sb^{3-})^{3+}$ model. In a real M_3Sb compound, included there are unoccupied metal atom p and d orbitals (above the Sb p orbital) accessible to bonding in the compound. Since in $D0_3$ symmetry the metal p and $M_{\rm II}$ d orbitals have an identical representation (Γ_{15}) to that of the Sb p orbitals, the two can interact. In this interaction, the (lower) bonding combination (i.e., the VBM) is pushed to lower energy; hence, the VBM is depressed relative to its value in the hypothetical $(Sb^{3-})^{3+}$ compound. This p-d repulsion has the following consequences.

(i) The band gaps of Cs_3Sb and K_3Sb are finite, whereas that of $(Sb^{3-})^{3+}$ at the respective lattice constants of

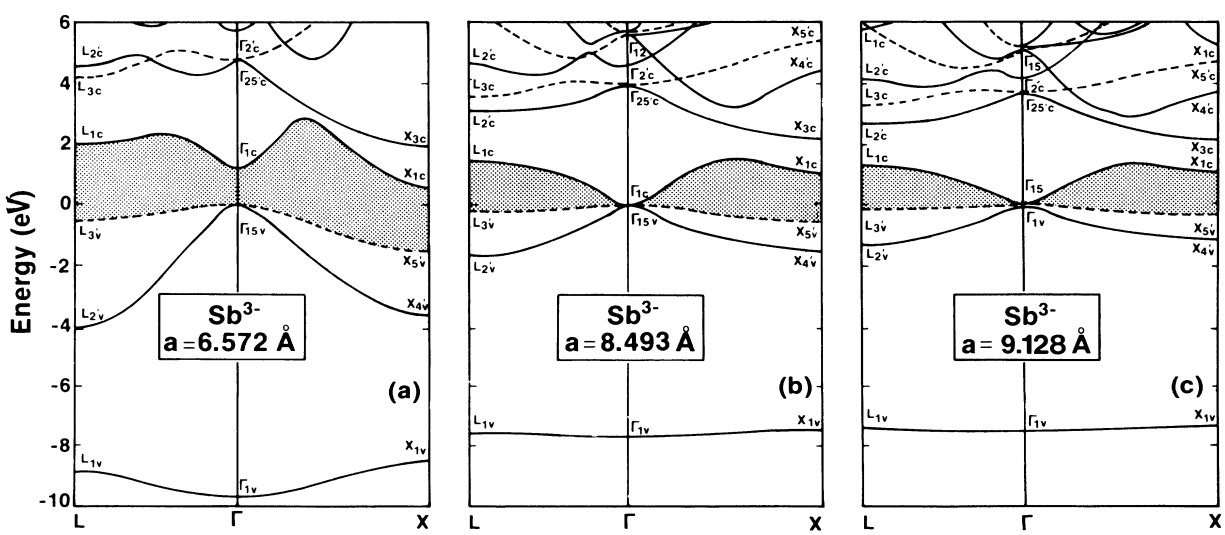

FIG. 4. Band structure of cubic Sb^{3-} (with three compensating positive charges) at the lattice constants of the respective M_3Sb compounds (a) $a=6.572$ Å, (b) $a=8.493$ Å, and (c) $a=9.128$ Å. The band-gap regions are shaded. Dashed lines indicate doubly degenerate states. The origin of the coordinate systems is at the Sb site.

TABLE III. Comparison of the bandwidths and band gaps of Li_3Sb, K_3Sb, Cs_3Sb with those obtained in a calculation for a fictitious Sb^{3-} lattice with three compensating (uniform background) positive charges at their respective lattice constants. All energies are in eV. W_{VB1} and W_{VB2} are the widths of the lower and upper valence bands; W_{tot} is the total valence-band width.

	$a=6.572$ Å		$a=8.493$ Å		$a=9.128$ Å	
Properties	Li_3Sb	Sb^{3-}	K_3Sb	Sb^{3-}	Cs_3Sb	Sb^{3-}
W_{VB1} (X_{1v}-Γ_{1v})	0.89	1.15	0.20	0.16	0.13	0.08
W_{VB2} (Γ_{15v}-$L_{2'v}$)	3.74	4.03	1.26	1.65	0.45	1.29
W_{tot} (Γ_{15v}-Γ_{1v})	9.31	9.69	7.31	7.66	6.94	7.45
E_g^D (Γ_{1c}-Γ_{15v})	2.20	1.23	0.56	0.04	1.02	−0.07
E_g^I (X_{1c}-Γ_{15v})	0.74	0.63	1.39	1.09	1.75	1.05

Cs_3Sb and K_3Sb nearly vanishes [Figs. 4(b) and 4(c)].

(ii) The (Sb p)-(Sb s) separation in K_3Sb and Cs_3Sb (Γ_{15v}-Γ_{1v}, or W_{tot} in Table III) is smaller than the value in the free Sb ion (8.08 eV) or in the hypothetical $(Sb^{3-})^{3+}$ system, due to this depression of Γ_{15v} by p-d and p-p repulsions.

(iii) The upper valence band (Γ_{15v}-$L_{2'v}$, or W_{VB2} in Table III) is narrower in the actual M_3Sb material since its low-lying empty d and p orbitals repel it.

(iv) The $X_{5'v}$ band in Cs_3Sb is *higher* than Γ_{15v} [the opposite situation prevails in $(Sb^{3-})^{3+}$ at the Cs_3Sb lattice constant], leading to an "inverted valence band," since the low-lying Cs d orbitals effectively depress the Γ_{15v} state.

(v) The spin-orbit splittings of the valence-band maximum (Δ_0 in Table I) are smaller for $M=K$ and $M=Cs$ than for $M=Li$ because of hybridization with metal d orbitals in $M=K$, Cs (d orbitals contribute to Δ_0 with opposite signs than p orbitals).

We tested our model of p-d repulsion by artificially removing the K $3d$ orbitals inside the muffin-tin spheres from the basis functions. We found that K_3Sb became metallic with an *inverted* band gap of −1.07 eV (i.e., Γ_{1c} was lower than Γ_{15v}), W_{tot} increased to 8.94 eV, and the calculated spin-orbit splitting Δ_0 became 0.62 eV, close to the Sb atomic value of 0.63 eV. This confirms the expected perturbative effects of cation p and d orbitals on the band structure of $(Sb^{3-})^{3+}$.

3. *Cation s orbital effects*

Within a pseudopotential picture, the effective s potential for valence electrons becomes shallower and more delocalized in the Li→Na→K→Rb→Cs series (see Fig. 5 in Ref. 33) due to pseudopotential cancellation effects. This is reflected in our all-electron results in an upwards shift in the s orbital energies (Table IV) and in a decrease in electronegativity (1.0, 0.8, and 0.7 for Li, K, and Cs, respectively, on Pauling's scale[34]). This trend has the following consequences.

(i) Cs transfers its s charge to Sb more effectively than do Li or K, resulting in an increased ionicity. Cs_3Sb tends to have a larger band gap based on the atomic orbital energies.

(ii) Relativistic effects, stronger for s than for p or d orbitals and increasing rapidly with atomic number, change the band structures of M_3Sb in proportion to the position of the metal s orbitals. For example, relativistic effects reduce the direct band gap ($\Gamma_{1c}\rightarrow\Gamma_{15v}$), because the Γ_{1c} state originates from the metal s states, and has therefore a larger relativistic lowering than the Γ_{15v} states, which have p character (even though the Γ_{15v} states are more localized). However, the reduction of band gap due to relativistic effects decreases with increasing lattice constant because the Γ_{1c} states become more delocalized.

The band gaps of the M_3Sb series are hence determined by a combination of (a) volume deformation effects [leading to $E_g(Li_3Sb)>E_g(K_3Sb)>E_g(Cs_3Sb)$], (b) p-d repulsion effect (depressing the VBM of Cs_3Sb more than that of K_3Sb or of Li_3Sb, hence acting in the opposite direction to volume deformation effects), and (c) ionicity effects (increasing the band gaps in the order Cs > K > Li). We find that effect (a) dominates Li_3Sb, which has the largest band gap in this series (despite its smaller ionicity relative to the other two), and that effects (b) and (c) (stronger in Cs than in K) are responsible for $E_g(Cs_3Sb)>E_g(K_3Sb)$.

4. *Electrostatic effects: The interstitial insertion rule*

The conduction bands of M_3Sb differ in a number of ways from those of $(Sb^{3-})^{3+}$. Wood *et al.*,[35] Carlsson *et al.*,[36] and Wei and Zunger[37] have advanced the "interstitial insertion rule," which explains such modifications in terms of the nature and amplitude (small or large) of conduction-band states at sites where atoms are interstitially introduced. This rule, specialized here for alkali atoms, states that conduction bands with s (p,d) character at interstitial site α are raised (lowered) when an alkali atom is introduced into site α. A number of such changes are related to this rule.

(i) The L_{3c} state of $(Sb^{3-})^{3+}$ at the lattice constant of Li_3Sb (a non-s state), is lowered by about 2 eV in Li_3Sb

TABLE IV. Calculated atomic orbital energies of Sb, Li, K, and Cs within the local-density formation. The energy zero is placed at Sb $5p$ states.

Atom	States	ε (eV)
Sb	$5s$	−8.08
	$5p$	0
Li	$2s$	2.12
K	$4s$	2.57
Cs	$6s$	2.78
	$5p$	−8.59

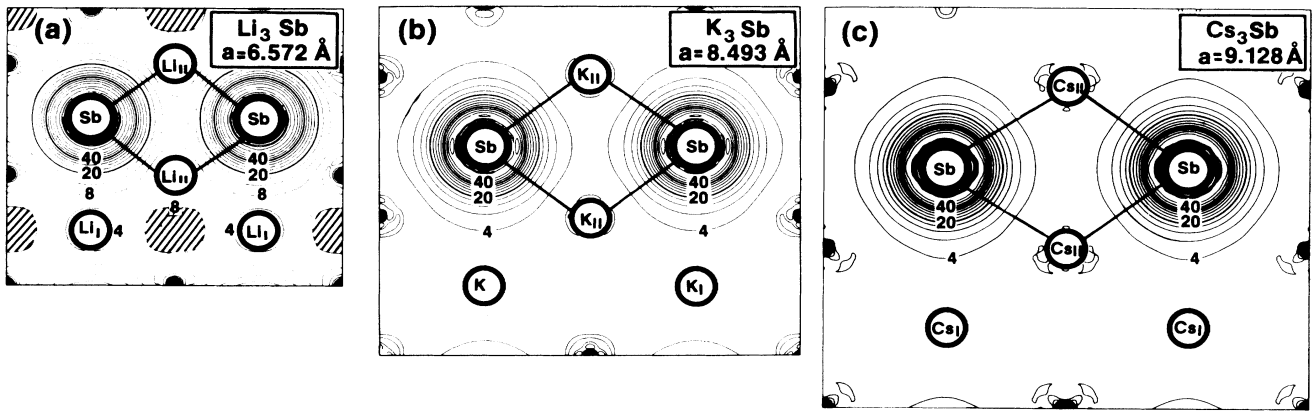

FIG. 5. Calculated valence charge-density contours (in units of 10^{-3} e/a.u.^{3}) for (a) Li_3Sb, (b) K_3Sb, and (c) Cs_3Sb (without Cs $5p$ states) on the (110) plane. Successive contours are separated by 4×10^{-3} e/a.u.^{3} Plots are drawn with the correct proportion of the lattice parameters. Dashed regions in (a) show Li-Li bond.

[compare Figs. 4(a) and 2(a)].

(ii) The strongly dispersive $\Gamma_{25'c}$- (a non-s state) X_{3c} (an s-like state) band in $(Sb^{3-})^{3+}$ with lattice constant of Li_3Sb is lowered (for $\Gamma_{25'c}$) and raised (for X_{3c}) in Li_3Sb, becoming dispersionless in real Li_3Sb [compare Figs. 4(a) and 2(a)].

(iii) In $(Sb^{3-})^{3+}$ at the lattice constant of Cs_3Sb, the X_{1c} (s-like) and X_{3c} (non-s-like in K_3Sb and Cs_3Sb due to the proximity of the metal d orbitals) are pushed upwards (for X_{1c}) and downwards (for X_{3c}) when Cs is introduced [compare Figs. 4(c) and 2(c)]. This explains the reversal of X_{1c} and X_{3c} states in Cs_3Sb relative to the corresponding $(Sb^{3-})^{3+}$.

Finally, since more electrons are lost from the $M_{\rm I}$ atom than from the $M_{\rm II}$ atom (because of the altered symmetry and the larger anion-cation distance for the $M_{\rm I}$ atom), a state centered on an $M_{\rm I}$ atom has a lower energy than the same state centered on an $M_{\rm II}$ atom. This implies that the $M_{\rm I}$ atom contributes more to the lower part of the conduction bands. This can be seen clearly from the DOS plot of Figs. 3(a)—3(c).

D. Charge densities and chemical bonding

Because it is somewhat arbitrary to define charges inside muffin-tin spheres (and from these ionicities) it is not sufficient to study the chemical bonding in this way alone. We have therefore plotted the charge densities of Li_3Sb [Fig. 5(a)], K_3Sb [Fig. 5(b)], and Cs_3Sb [Fig. 5(c)] in the (110) plane at their experiment lattice constants. For Li_3Sb we find that the chemical bonding between $M_{\rm II}$ and the Sb atom is partially ionic and partially covalent with larger ionic character. (Because of the delocalized nature of the Sb $5p$ states, this ionic character is often obscured by looking only at the total change contained within atom-centered spheres.) We also find that there is considerable covalent bonding in the cation-cation bonds [dashed region in Fig. 5(a)] and anion-anion bonds due to the small lattice constant. This can be seen even more clearly in Fig. 6(a) (dashed region), which shows the charge density along the [111] direction. For K_3Sb and Cs_3Sb, with larger lattice constants and an increased repulsiveness of the s potential,[33] more charge is

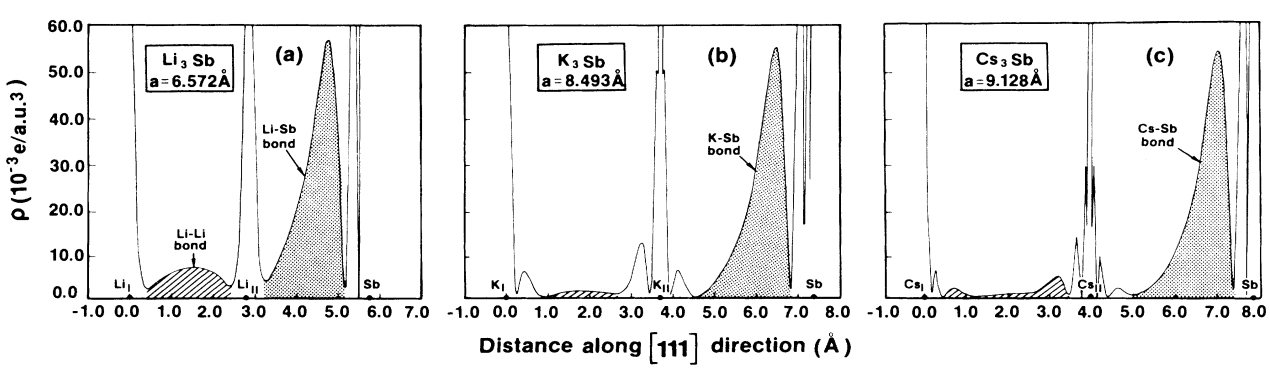

FIG. 6. Charge-density (in units of 10^{-3} e/a.u.^{3}) plots along the $M_{\rm I}$-$M_{\rm II}$-Sb bond for (a) Li_3Sb, (b) K_3Sb, and (c) Cs_3Sb. Shaded (dashed) regions show M-Sb (M-M) bonds.

transferred to the Sb atom, hence the covalent bonding becomes weaker for both like atoms and unlike atoms (it almost disappears in Cs_3Sb). As more charge is transferred to the Sb atom, the Sb $5p$ states become even more extended. These trends can be seen clearly in Figs. 6(b) and 6(c). Our results, therefore, indicate that in M_3Sb, like atoms (M-M, Sb-Sb) tend to have covalent bonds and M-Sb interactions tend to be ionic. This is reasonable considering the large electronegativity differences between the alkali metals and Sb atom. The longer the bond length, the more the charge transfer. For Cs_3Sb, we find that Cs exists predominantly in the $Cs^{+(1-\varepsilon)}$ form (where ε is a small positive number due to the attractive singularity of the Coulomb potential near the nuclei). Our results therefore support the conclusion drawn from the photoemission measurements of Bates *et al.*[13] that Cs atoms in Cs_3Sb are predominantly in the Cs^+ form. The half covalent, half ionic model[15] is not valid for Cs_3Sb, but is approximately true for Li_3Sb due to the smaller lattice constant. Our interpretation is also similar to that of Robertson[10] except that his definition of ionicity is vitiated for smaller bond length because of the delocalized Sb $5p$ orbitals.

IV. CONCLUSION

We have calculated the ground state properties at $T=0$ K and the electronic band structures of the alkali-antimony compounds Li_3Sb, K_3Sb, and Cs_3Sb. The ground-state properties obtained by minimizing the total energy are in good agreement with experiment. For Cs_3Sb we find that correct treatment of the partially delocalized Cs $5p$ states is necessary to obtain the correct lattice constant. Electronic structure calculations for M_3Sb demonstrate that these systems can be considered to low order as an Sb^{3-} lattice with its lattice constant determined by the alkali atom cores. Insertion of the alkali ions into the hypothetical Sb^{3-} sublattice interstitial sites can be treated as a perturbation: the relative shift of the eigenvalues upon insertion can be understood in terms of (i) p-d repulsion, (ii) cation s orbital effects (including relativistic effects), and (iii) the "interstitial insertion rules." We find the maxima of valence band for K_3Sb and Cs_3Sb are very flat and structureless, a property which may be responsible for the high photoelectric efficiency of this system (besides the surface induced effects), especially for Cs_3Sb. The interaction between the Sb $5p$ states and the unoccupied alkali d states is found to be responsible for the semiconducting properties and flatness of the upper valence band. Calculated charge-density maps indicate that like atoms in M_3Sb tend to have covalent bonding and unlike atoms tend to have ionic bonding. With increasing lattice constant the covalency decreases but the ionicity increases. We find Li_3Sb has both covalent bonding and ionic bonding but Cs_3Sb is almost purely ionic.

ACKNOWLEDGMENTS

We thank D. M. Wood for his comments on this paper. This work was supported by the Office of Energy Research, Materials Science Division, U.S. Department of Energy, Grant No. DE-AC02-77-CH00178.

[1]For a comprehensive review, see A. H. Sommer, *Photoemissive Materials* (Wiley, New York, 1968).
[2]P. Görlich, Z. Phys. **101**, 335 (1936).
[3]W. E. Spicer, Phys. Rev. **112**, 114 (1958).
[4]G. Brauer and E. Zintl, Z. Phys. Chem. **37B**, 323 (1937).
[5]A. H. Sommer and W. H. McCarroll, J. Appl. Phys. **17**, 1005 (1966).
[6]K. H. Jack and M. M. Wachtel, Proc. R. Soc. London, Ser. A **239**, 46 (1957).
[7]A. Blancher, H. Presting, and M. Cardona, Phys. Status Solidi B **126**, 11 (1984).
[8]A. A. Mostovskii, V. A. Chaldyshev, V. P. Kiselev, and A. I. Klimin, Izv. Akad. Nauk SSSR. Ser. Fiz. **40**, 2490 (1976) [Bull Acad. Sci. USSR, Phys. Ser. **40**, 36 (1976)]; A. A. Mostovskii, V. A. Chaldyshev, and G. F. Karavaer, A. I. Klimin, and I. N. Ponomarenko, *ibid.* **38**, 195 (1974) [*ibid.* **38**, 10 (1974)].
[9]F. Wooten, J. P. Hernandez, and W. E. Spicer, J. Appl. Phys. **44**, 1112 (1973).
[10]J. Robertson, Phys. Rev. B **27**, 6322 (1983).
[11]N. E. Christensen, Phys. Rev. B **32**, 207 (1985).
[12]R. Dupree, D. J. Kirby, and W. Freyland, Z. Naturforsch. **37A**, 15 (1982).
[13]C. W. Bates, Jr., D. D. Gupta, L. Galan, and D. N. E. Buchanan, Thin Solid Films **69**, 175 (1980).
[14]H. Redslob, G. Steinleitner, and W. Feyland, Z. Naturfosch. **37A**, 587 (1982).
[15]J.-P. Suchet, Acta Crystallogr. **14**, 651 (1961).
[16]A. Nishikawa, K. Niizeki, K. Shindo, and H. Tanaka, J. Phys. Soc. Jpn. **54**, 4059 (1985).
[17]S.-H. Wei, H. Krakauer, and M. Weinert, Phys. Rev. B **32**, 7792 (1985), and references therein.
[18]P. Hohenberg and W. Kohn, Phys. Rev. **136**, 864 (1964); W. Kohn and L. J. Sham, *ibid.* **140**, 1133 (1965).
[19]E. Wigner, Phys. Rev. **46**, 1002 (1934).
[20]L. Hedin and B. I. Lundquist, J. Phys. C **4**, 2064 (1971); V. Von Barth and L. Hedin, *ibid.* **5**, 1629 (1972).
[21]J. Perdew and A. Zunger, Phys. Rev. B **23**, 5048 (1981).
[22]D. J. Chadi and M. L. Cohen, Phys. Rev. B **8**, 5747 (1973).
[23]O. Jepsen and O. K. Andersen, Solid State Commun. **9**, 1763 (1971); G. Lehman and M. Taut, Phys. Status Solidi **54**, 469 (1972).
[24]*Landolt-Börnstein Numerical Data and Functional Relationships in Science and Technology,* edited by O. Madelung (Springer-Verlag, Berlin, 1982), Vol. 17e, p. 126–135; *ibid.* Vol. 17b; *ibid.* edited by O. Madelung, M. Schulz, and H. Weiss (Springer-Verlag, Berlin, 1982), Vol. 17a.
[25]Heat of formation at 298 K is from O. Kubachevski and C. B. Alcock, in *Metallurgical Thermochemistry,* 5th ed. (Pergamon, New York, 1979); cohesive energies for elements at 0 K are taken from C. Kittel, *Solid State Physics,* 5th ed. (Wiley, New York, 1976).

[26]Treatment (1) of Table IV of Ref. 17 was used here. The larger lattice constants obtained by Christensen (Ref. 11) (cf., Table I), especially for Cs_3Sb, are probably due to the use of the renormalized frozen-core approximation. Such an approximation has been known (see Ref. 17) to exaggerate the lattice parameter, particularly when one renormalizes and freezes the rather extended Cs $5p$ orbitals.

[27]S.-H. Wei and H. Krakauer (unpublished).

[28]R. Gobrecht, Phys. Status Solidi **13**, 429 (1966).

[29]N. E. Christensen (private communication).

[30]A. Ebina and T. Takahashi, Phys. Rev. B **7**, 4712 (1973).

[31]G. Wallis, Ann. Phys. **17**, 401 (1956).

[32]R. Zallen and W. Paul, Phys. Rev. **134**, A1628 (1964); G. A. Samara, Phys. Rev. B **27**, 3494 (1983).

[33]A. Zunger and M. L. Cohen, Phys. Rev. B **18**, 5449 (1978).

[34]L. Pauling, *The Nature of the Chemical Bond* (Cornell University Press, Ithaca, N.Y., 1960).

[35]D. M. Wood, Alex Zunger, and R. DeGroot, Phys. Rev. B **31**, 2570 (1985).

[36]A. Carlsson, A. Zunger, and D. Wood, Phys. Rev. B **32**, 1386 (1985).

[37]S.-H. Wei and Alex Zunger, Phys. Rev. Lett. **56**, 528 (1986).